SEMI-ANNUAL STATUS REPORT

February 1986 - July 1986

for

NASA Grant NSG 1419

THE STRUCTURE OF SEPARATED FLOW REGIONS OCCURRING NEAR THE LEADING EDGE OF AIRFOILS INCLUDING TRANSITION

Thomas J. Mueller
Principal Investigator

Department of Aerospace and Mechanical Engineering
University of Notre Dame
Notre Dame, Indiana 46556

July 1986

SEMI-ANNUAL STATUS REPORT

February 1986 - July 1986

for

NASA Grant NSG 1419*

The majority of the time and effort during this report period was directed toward analyzing the hot-wire anemometer data already acquired. Additional static pressure distributions and flow visualization data were acquired to help with the analysis of the velocity profile data.

This research has as its objective the detailed documentation of the structure and behavior of the separation bubble including transition and the redeveloping boundary layer after reattachment over an airfoil at low Reynolds numbers. The intent of this work is to further the understanding of the complex flow phenomena so that analytic methods for predicting their formation and development can be improved. These analytic techniques have applications in the design and performance prediction of airfoils operating in the low Reynolds number flight regime.

Efficient subsonic performance of airfoils at chord Reynolds numbers on the order of 100,000 may be required for remotely piloted aircraft. Several problems have arisen, however, in the development of such airfoils. For example, conventional design strategies seek to control the onset and development of turbulent boundary layers. This becomes difficult at low Reynolds numbers due to the increased stability of laminar boundary layers.

---

* NASA Technical Monitor for this Grant is
Mr. Dan M. Somers, NASA Langley Research Center
Hampton, Virginia 23665.

The development of a turbulent boundary layer under these conditions may depend on the formation of a transitional separation bubble. This flow phenomenon, shown in Figure 1, involves the separation of a laminar boundary layer, followed by transition of the highly unstable separated shear layer. Turbulent mixing then results in reattachment of the shear layer. However, the turbulent boundary layer which develops downstream of the separation bubble is usually thicker than one formed in an attached transition process. This results in higher drag. Furthermore, the separation bubble can have a great effect on an airfoil's stalling characteristics. Therefore, airfoil design/analysis methods must be able to predict the influence of separation bubbles.

REVIEW OF PREVIOUS SEPARATION BUBBLE METHODS OF ANALYSIS

In order to account for the effects of a separation bubble, at least two things must be known. First, the location of turbulent reattachment is needed as the starting point for computing the development of the turbulent boundary layer along an airfoil's surface. This, in turn, requires knowledge of the position of laminar separation and of the extent of the bubble's laminar and turbulent portions. Second, the boundary layer characteristics at reattachment are needed such as δ_2, U, H_{12} and H_{32}. These would be used as initial conditions in a turbulent boundary layer computation scheme.

A rather simple method exists which is capable of estimating the extent of a separation bubble and the conditions at reattachment. This method was developed by H.P. Horton [Ref. 1] in order to explain the breakdown of separation bubbles. Later, it was employed by Roberts to predict the effect of separa-

tion bubbles on airfoil performance [Ref. 2]. A similar approach was devised by Vincent de Paul to predict the stalling behavior of airfoils [Ref. 3]. A broad description of Horton's method is that it provides a set of relationships which describe the characteristics of a separation bubble in terms of boundary layer parameters obtained at the laminar separation point. This was accomplished through an analysis of the integral forms of the momentum and kinetic energy equations coupled with simplifying assumptions concerning the external velocity distribution and the flow within a bubble.

The assumed form of the external velocity distribution is shown in Figure 2. The perturbation due to the displacement of the external flow by the bubble is confined to the region between laminar separation and turbulent reattachment. Downstream of separation, the velocity was considered to be constant until transition occurred. In the turbulent portion of the bubble, the external velocity was assumed to decrease linearly with distance from the value of transition (= U_s) to that at reattachment.

Horton characterized the flow within the laminar recirculation region of a bubble as essentially stagnant. He then argued that the skin friction was negligible as a result. In addition, according to his assumed external velocity distribution, dU/ds=0. From the momentum integral equation given below,

$$d\delta_2/ds + (H_{12} + 2)\,(\delta_2/U)(dU/ds) = C_f/2 \qquad (1)$$

one finds that $d\delta_2/ds$ is equal to zero. Therefore, the momentum thickness at transition must be the same as at separation. The length of the bubble's laminar region, l_1, was determined using the following relationship

$$l_1/(\delta_2)_S = R_{l_1}/(R_{\delta_2})_S \qquad (2)$$

where the transition Reynolds number, R_{l_1}, was assumed to be invarient and equal to 40,000. Thus, by using a conventional boundary layer method, the location and characteristics (such as U, δ_2, R_{δ_2}) corresponding to laminar separation could be found. From this information, the extent of laminar separated flow and the momentum thickness at transition immediately followed.

In the turbulent portion of a bubble, neither dU/dS nor C_f can be neglected. As a result, Equation 1 cannot be easily evaluated. Instead, Horton used this form of the kinetic energy integral equation:

$$d(U^3\delta_3)/ds = C_d\, U^3 \tag{3}$$

in which the contribution due to the normal Reynolds stresses has been neglected. The energy thickness δ_3 was then expressed as the product of H_{32} and δ_2. Since H_{32} remains essentially constant in regions of separated flow (approximately equal to 1.5), Equation 3 could be integrated from the point of transition to reattachment in order to determine the growth in δ_2:

$$U_R^3(\delta_2)_R - U_T^3(\delta_2)_T = \frac{1}{H_{32}} \int_{s_T}^{s_R} C_d\, U^3 ds \tag{4}$$

In this expression, U_T and $(\delta_2)_T$ were known (being equal to the values at separation). In addition, the variation in U between s_T and s_R was assumed to be

$$U = U_S + (U_R - U_S)(s - s_T)/l_2 \tag{5}$$

although U_R and l_2 were still unknowns. In order to perform the integration in Equation 4, the dissipation coefficient C_d had to be determined. This parameter is defined as:

$$C_d = 2/\rho U^3 \int_0^{\delta} \tau \partial u/\partial y \; dy \qquad (6)$$

where $\tau = -\rho u' v' + \mu \partial u/\partial y$ for turbulent flow. Obviously, the dissipation coefficient depends on the shape of the velocity profile. Since the profile shapes will vary from transition to reattachment, C_d can also be expected to change. Instead of allowing C_d to vary with s, however, Horton decided to use a mean value, C_{d_m} to represent the dissipation coefficient in a bubble's turbulent region. For C_{d_m}, he chose 0.0182 which corresponded to C_d for an asymptotic mixing layer. Roberts, on the other hand, argued that this value was not appropriate for reattaching turbulent flows since it was based on a flow with zero pressure gradient. He found, from measurements of separation bubbles, an average value of 0.035 for C_{d_m} [Ref. 4].

Taking mean values for H_{32} and C_d, Equation 4 can be integrated, yielding

$$(\delta_2)_R = (\delta_2)_T (U_T/U_R)^3 + (C_d/H_{32})_m (1 + U_T/U_R)[1 + (U_T/U_R)^2]l_2/4 \qquad (7)$$

In order to compute the momentum thickness at reattachment, however, U_R and l_2 are required. These quantities can be determined using Horton's reattachment criterion. By combining the momentum and the kinetic energy integral equations and utilizing the characteristics of a reattaching velocity profile ($C_f = 0$, $dH_{32}/dH_{12} \approx 0$), he derived the following equation:

$$(\delta_2/U)(dU/ds) = - C_d/[H_{32}(H_{12}-1)] \qquad (8)$$

which must be satisfied at the point of reattachment. Furthermore, he argued that the right-hand side of this expression depends only on the shape of the velocity profile. Finally, he examined several reattaching profiles and found

that they were nearly identical. Thus, the right-hand side of Equation 8 was shown to be a constant which implied that

$$[(\delta_2/U)\bullet(dU/ds)]_R = \Lambda_R \tag{9}$$

where Λ_R is a constant which Horton estimated would equal -0.00592. Data obtained from 22 experiments involving separation bubbles as well as flow reattaching downstream of backward-facing steps and roughness elements indicated a range of values from -0.0057 to -0.0109, however. After examining the distribution of this data and finding it corresponded fairly well to the normal distribution curve, he concluded that the variation was due to random error in the experiments and selected the mean value of -0.0082 as his reattachment criterion. Roberts examined additional measurements and calculated a new mean (including Horton's data) of -0.0075 [Ref. 4].

In applying the reattachment criterion, the external velocity gradient was presumed by Horton to equal $(U_R-U_T)/l_2$. By combining Equations 7 and 9, a formula for l_2 can be obtained:

$$l_2 = (\delta_2)_T\,(U_T/U_R)^3\,(1-U_T/U_R)/\{\Lambda_R + (C_d/H_{32})_m[(U_T/U_R)^4-1]/4\} \tag{10}$$

Reattachment corresponds to the point at which the curve describing s_R as a function of U_R first intersects the external velocity distribution with the bubble absent. Therefore, a sort of viscous-inviscid interaction is involved. On the one hand, the external velocity distribution in the bubble's turbulent region governs the growth of the separated shear layer. On the other hand, for reverse flow to be eliminated at the designated reattachment point, the pressure distribution must satisfy Equation 9. This criterion implies the

simultaneous satisfaction of the momentum and kinetic energy integral equations at the location of turbulent reattachment.

Once the reattachment point is established, the momentum thickness follows from Equation 7. Since the velocity profile is universal at reattachment (according to Horton), the shape parameters are known (H_{12} = 3.5, H_{32} = 1.51). Thus, a turbulent boundary layer calculation can be initiated using these characteristics as initial conditions.

LOW REYNOLDS NUMBER SEPARATION BUBBLE ANALYSIS

Horton's semi-empirical method is appealing because it allows one to calculate separation bubble characteristics very easily. However, its reliance on experimental data limits its applicability. The goal of the present study was to evaluate the assumptions on which Horton's theory was based under low Reynolds number conditions. This goal was achieved by examining measurements of separation bubbles formed on an NACA 66_3-018 airfoil at chord Reynolds numbers ranging from 50,000 to 200,000 [Ref. 5]. This data consisted of hot-wire velocity profiles measured at 20 or 24 stations along the upper surface of the airfoil when it was at angles of attack of 10 and 12 degrees. Measurements were also obtained in different freestream disturbance environments. In order to modify the disturbance environment within the wind tunnel, flow restricting devices were introduced downstream of the test section. Each flow restrictor consisted of a wooden frame (with the same width and height as the test section) packed with plastic drinking straws. The introduction of flow restrictors resulted in a higher freestream turbulence level at a given speed. Table 1 lists representative turbulence intensities at the test con-

ditions.

The velocity profiles were obtained using a single hot-wire sensor. Thus, only velocity magnitudes were measured. Now, the locations of separation and reattachment are interfaces between regions of forward and reverse flow. Therefore, the hot-wire probe's inability to indicate flow direction complicates the determination of these locations. Also without precise knowledge of the flow direction, the integral parameters (δ_1, δ_2, δ_3, H_{12} and H_{32}) could not be accurately determined. For example, consider the velocity profile in Figure 3. The height of the dividing streamline, which defines the extent of recirculating flow, is y_{DS}. The resulting momentum thickness is defined as:

$$\delta_2 = \int_o^{\delta} u/U(1-u/U)dy \tag{11a}$$

$$= \int_o^{y_{DS}} u/U\, dy + \int_{y_{DS}}^{\delta} u/U\, dy - \int_o^{\delta} (u/U)^2 dy \tag{11b}$$

The first integral is zero since it defines the net mass flow of the recirculation region. However, if u/U is treated as positive across the layer, this integral will not equal zero and δ_2 will be found to be larger than it actually is. The energy thickness δ_3 will also experience a fictitious growth. The displacement thickness δ_1, however, would be reduced.

In order to eliminate these errors, a technique was sought which could determine the height of the dividing streamline y_{DS} from the experimental velocity profiles. From Equation 11b, it was noticed that as y increases, δ_2 decreases. Since the quantity δ-y_{DS} also decreases, it was hypothesized that the ratio $(\delta-y_{DS})/\delta_2$ might remain constant. This hypothesis was tested by computing this ratio for a variety of analytical reverse flow velocity pro-

files (with δ = y at which u/U = 0.99). The results are shown plotted against H_{12} in Figure 4. In general, the ratio of the separated shear layer thickness to the momentum thickness varies a great deal with H_{12}. However, in the range of H_{12} appropriate for separation bubbles (from about 3 to 11), this ratio is approximately constant and equal to 7. Linear fits for this data are given below:

$$\Delta y/\delta_2 = 4.9410 + 0.2534\ H_{12}, \quad 3.00 < H_{12} < 137.50 \tag{12a}$$

$$\Delta y/\delta_2 = 0.7384 + 0.2418\ H_{12}, \quad -81.25 < H_{12} < -3.00 \tag{12b}$$

where Δy is the distance from the dividing streamline to the point at which u/U = 0.99. These equations were then used to determine y_{DS} for experimental velocity profiles in the vicinity of separation bubbles. It was assumed that y_{DS} coincided with the data point in each profile for which H_{12} and $\Delta y/\delta_2$ best satisfied Equation 12a or 12b. The resulting streamline shapes are shown in Figures 5 through 8. In figure 9, the importance of taking reverse flow into account when computing δ_1 and δ_2 can be seen.

Upon examination of the corrected hot-wire data, a significant growth in δ_2 was noticed in the laminar portion of each separation bubble. This was of particular interest since Horton had concluded that δ_2 remains constant between separation and transition. For a two-dimensional laminar half-jet, the theoretical momentum thickness growth is,

$$\frac{\delta_2}{(\delta_2)_o} = \sqrt{\frac{1.4326\ (x-x_o)}{(\delta_2)_o (R_{\delta_2})_o} + 1} \tag{13}$$

which was derived from the solution in Reference 6. In this expression, the subscript "o" designates a quantity at some reference location. For a separa-

tion bubble, this location is clearly the separation point. Figure 10 shows $\delta_2/(\delta_2)_S$ plotted against $(s-s_S)/(\delta_2)/(R_{\delta_2})_S$. Despite some scatter, the data tends to collapse along a single curve. For values of the parameter $(s-s_S)/(\delta_2)_S/(R_{\delta_2})_S$ less than 6, Equation 13 represents the momentum thickness growth fairly well. For larger values of this parameter, the equation underpredicts the growth. Perhaps this is indicating that viscous diffusion is no longer the only mechanism for shear layer growth. The appearance of Reynolds stresses in a region of transitioning flow may account for some of the increase in δ_2.

The discrepancy between Horton's conclusion concerning momentum thickness growth and the present results may be answered in several ways. Vincent de Paul attributed this discrepancy to neglected terms in the momentum equation; in particular, one resulting from a pressure gradient across the separated flow [Ref. 3]. However, no such gradient is present in the planar half-jet flow, yet a momentum thickness growth still occurs. Perhaps the only conclusion one can derive from the momentum integral equation is that, since C_f and dU/ds are very small, $d\delta_2/ds$ must be very small as well. This is a substantially different conclusion than Horton arrived at, for d_{δ_2}/ds may be written in the following form:

$$d\delta_2/ds = d[\delta_2/(\delta_2)_S]/d[s/(\delta_2)_S] \tag{14}$$

If it is assumed that $d\delta_2/ds$ is constant over the bubble's laminar portion, one finds that

$$d\delta_2/ds = [(\delta_2)_T/(\delta_2)_S - 1]/[l_1/(\delta_2)_S] \tag{15}$$

Since $l_1/(\delta_2)_S$ is on the order of 100 to 300 [Ref. 1], $(\delta_2)_T$ could be larger than $(\delta_2)_S$ without violating the observation that $d\delta_2/ds$ be small. Further,

by employing Equation 2, Equation 15 becomes:

$$d\delta_2/ds = (R_{\delta_2})_S \left[(\delta_2)_T/(\delta_2)_S - 1\right]/R_{l_1} \qquad (16)$$

Thus, larger increases in momentum thickness are allowed as $(R\delta_2)_S$ becomes smaller. Since $(R\delta_2)_S$ is proportional to $R_c^{1/2}$, this suggests that a substantial growth might occur in the laminar portion of a bubble formed on a low Reynolds number airfoil.

These conclusions can also be obtained from Equation 13. If the parameter, $l_1/(\delta_2)_S/(R_{\delta_2})_S$ is written in the form $Rl_1/(R\delta_2)_S^2$, it is seen that momentum thickness growth depends a great deal on $(R_{\delta_2})_S$ (or R_c). For example, if R_{l_1} = 40,000 and $(R_{\delta_2})_S$ = 500, $(\delta_2)_T$ will differ from $(\delta_2)_S$ by only 10.9 percent. This is probably within the uncertainty of experimental data. If $(R_{\delta_2})_S$ = 50, however, $(\delta_2)_T/(\delta_2)_S$ = 4.89. Thus, Horton's conclusion appears to be a high Reynolds number approximation.

Horton's use of a constant value for the transition Reynolds number R_{l_1} may also be called into question. Dryden's review of research performed prior to 1955 does not provide any support for the universality of this parameter [Ref. 7]. He reported that R_{l_1} could take on values from 0 to 380,000, "..an even wider range than observed for the boundary layer on a plate without pressure gradient." The data which formed the basis for this review came from tests involving a variety of models, including circular and elliptic cylinders as well as airfoils ranging in t/c from 0.09 to 0.18. This would seem to imply that the pressure distribution plays a role in determining R_{l_1}. This observation is strengthened by the airfoil experiments of Gault [Ref. 8] in which the transition Reynolds number varied by as much as a factor of 4 over

an angle of attack range of 8 degrees. Another factor which has been considered an important influence on R_{l_1} is the nature of turbulent fluctuations in the freestream; i.e., intensity and scale. A few correlations have been proposed which require R_{l_1} to be a function of these quantities; however, they have not been completely successful.

Although the concept of a constant transition Reynolds number is attractive because the length of a bubble's laminar region can be estimated directly from the conditions at separation, its lack of constancy limits its usefulness. On the other hand, a constant value of R_{l_1} would imply that, at low chord Reynolds numbers, a separation bubble would occupy most of the airfoil's surface (unless U_s/U_∞ was very large). Experimental evidence does not support this conclusion, however. Another argument against the concept of a constant transition Reynolds number is made apparent by Equation 2. It implies that a finite length of laminar separated flow will exist even for very large, but finite, values of $(R_{\delta_2})_S$. This implication is at odds with the conclusion of Crabtree that a value of $(R_{\delta_2})_S$ exists for which transition will take place at the separation point [Ref.9].

Estimates of R_{l_1} were obtained from O'Meara's data by assuming that transition took place at the end of the external velocity plateau. The resulting values for R_{l_1} are shown plotted against R_c in Figure 11. When no flow restrictors are present, the transition Reynolds number is approximately 20,000, only one-half the value used by Horton. The addition of one flow restrictor causes R_{l_1} to decrease by about 25 percent. When two flow restrictors are present, R_{l_1} is reduced an additional 20 percent. Obviously, the freestream disturbance environment is affecting the magnitude of R_{l_1}. It is

difficult to believe, however, that the disturbance environment is alone responsible for the large difference between Horton's value for R_{l_1} and O'Meara's data when no flow restrictors were present. After all, the turbulence level at these conditions was only on the order of 0.1 percent. Data obtained by Ntim at freestream turbulence levels less than about 0.45% yielded values of R_{l_1} ranging from 30,000 to 50,000 [Ref. 10]. However, $(R_{\delta 2})_S$ ranged from 271 to 414 for this data [Ref. 4]; whereas for O'Meara's data, $(R_{\delta 2})_S$ was between 28 and 100. Hence, it is possible that the transition Reynolds number may depend on $(R_{\delta 2})_S$. This possibility has been suggested by other researchers [Refs. 3 and 11]. Since $(R_{\delta 2})_S$ is affected by the pressure distribution, the idea that R_{l_1} depends on $(R_{\delta 2})_S$ would explain the effect of model shape on R_{l_1} noted earlier.

The growth in δ_2 over the turbulent portion of separation bubbles has also been evaluated. Comparisons between the predicted growth, using Equation 7, and the growth obtained from O'Meara's results are shown in Figure 12. Apparently, Horton's recommended value for $(Cd/H_{32})_m$ (= 0.0182/1.5 = 0.0121) is too small to predict $(\delta_2)_R/(\delta_2)_T$ accurately. In Figure 13, a similar comparison is made, this time using Robert's value for $(Cd/H_{32})_m$ (= 0.035/1.5 = 0.0233). In this case, $(\delta_2)_R/(\delta_2)_T$ is predicted much better. There is still a fair amount of scatter (with errors less than about $\pm$ 18%), however, the accuracy may be sufficient for engineering purposes.

Values for Horton's reattachment criterion have been derived from O'Meara's data and are shown plotted versus $(R_{\delta 2})_R$ in Figure 14. Included in the figure is Horton's original data base with a mean value of -0.0082 for Λ_R. O'Meara's data has a mean value of -0.0078 which lies between the values for

Λ_R determined by Horton and Roberts. The fairly large scatter in the data may be due to uncertainties in the exact location of reattachment since both δ_2 and U are changing rapidly in the vicinity of the reattachment point. Despite the scatter, it appears that Horton's reattachment criterion has been substantiated under low Reynolds number conditions.

In order to verify Horton's description of the characteristics at reattachment, i.e., $(H_{12})_R$ and $(H_{32})_R$, three velocity profiles were evaluated. These profiles were selected because they were obtained at locations very close to the presumed reattachment points. The three profiles have been plotted in Figure 15 along with Horton's mean reattachment profile. The profiles are quite different from Horton's curve, having much higher velocities near the airfoil's surface. As a result, $(H_{12})_R$ is about 2.8 instead of 3.5 as suggested by Horton. Of course, Horton's velocity profile looks more like one which would occur at reattachment since the skin friction is clearly zero. However, Thwaites [Ref.12] showed a turbulent separation profile which looks very much like O'Meara's profiles (Figure 16).

In Figure 17, the values of $(H_{12})_R$ and $(H_{32})_R$ taken from O'Meara's data are shown. Although $(H_{32})_R$ is close to 1.5, no single value exists for $(H_{12})_R$. Thus, it is only coincidental that the three velocity profiles discussed earlier had nearly the same value of H_{12}. At present, it is difficult to make any definite statements concerning $(H_{12})_R$. It is possible that there is no universal reattachment profile. However, it is also possible that the variations in H_{12} are due to measurement error. Because of the hot-wire probe's inability to sense flow direction, errors in the magnitude of both the mean and fluctuating velocity components can occur. This will happen whenever

the absolute vaule of the fluctuating component is larger than that of the mean. Thus, a measurement error of this type is likely to be confined near a solid boundary where the mean component is small. This is precisely the region in which the discrepancy between Horton's mean profile and O'Meara's profiles is the most noticeable. Since Horton's profile is based on measurements in which flow direction was determined, one would tend to have more confidence in his results.

CONCLUSIONS

A semi-empirical method for predicting separation bubble characteristics has been evaluated using low Reynolds number test data. On the basis of this data, several observations were made. First of all, a sizable growth in the momentum thickness can occur in the laminar portion of a separation bubble. This is in direct contrast to the theory and is apparently due to low Reynolds number effects. Secondly, the transition Reynolds number, R_{l_1}, which governs the extent of a bubble's laminar region, was found to be much lower than that used in the method. At present, there does not seem to be any evidence supporting a single value for R_{l_1}. Apparently, R_{l_1} is affected by the freestream disturbance environment, an airfoil's pressure distribution, and possibly the chord Reynolds number as well. Thirdly, the growth in momentum thickness over a bubble's turbulent region was predicted reasonably well by the method, provided that Roberts' suggested value for the mean dissipation coefficient was used. Finally, the present data does not substantiate the universality of the velocity profile at reattachment. However, measurement error may be responsible for this result.

REFERENCES

1. Horton, H.P., "Laminar Separation Bubbles in Two and Three Dimensional Incompressible Flow," Ph.D. Thesis, University of London, 1968.

2. Roberts, W.B., "Calculation of Laminar Separation Bubbles and Their Effect on Airfoil Performance," AIAA 79-0285, 1979.

3. Vincent de Paul, M., "Prevision du Decrochage d'un Profil d'Aile en Ecoulement Incompressible," AGARD-CP-102, 1972.

4. Roberts, W.B., "A Study of the Effect of Reynolds Number and Laminar Separation Bubbles on the Flow Through Axial Compressor Blades," DSc Thesis, U. Libre de Bruxelles, Institut d'Aeronautique, and von Kármán Institute for Fluid Dynamics, May 1973.

5. O'Meara, M.M., "An Experimental Investigation of the Separation Bubble Flow Field Over an Airfoil at Low Reynolds Numbers," M.S. Thesis, University of Notre Dame, 1985.

6. Schlicting, H., Boundary Layer Theory, McGraw-Hill, Inc., 1979.

7. Dryden, H.L., "Transition from Laminar to Turbulent Flow," Turbulent Flows and Heat Transfer, Princeton University Press, Princeton, New Jersey, 1959.

8. Gault, D.E., "An Experimental Investigation of Regions of Separated Laminar Flow," NACA TN3505, 1955.

9. Crabtree, L.F., "Prediction of Transition in the Boundary Layer on an Aerofoil," Journal of the Royal Aeronautical Society, Volume 62, July 1958, pp. 525-528.

10. Young, A.D., "Some Special Boundary Layer Problems," Z. Flugwiss Weltraumforsch. 1, Heft 6, 1977, pp. 401-414.

11. Woodward, D.S., "An Investigation of the Parameters Controlling the Behaviour of Laminar Separation Bubbles," Royal Aircraft Establishment Technical Memorandum Aero 1003, August 1967.

12. Thwaites, B., Incompressible Aerodynamics, Oxford at the Clarendon Press, 1960.

NOMENCLATURE

c	Airfoil chord
C_d	Dissipation coefficient, $2/\rho U^3 \int_0^{\delta} \tau \, \partial u/\partial y \; dy$
C_f	Skin friction coefficient, $2/\rho U^2 \, \tau\|_{y=0}$
H_{12}	Boundary layer shape parameter, δ_1/δ_2
H_{32}	Boundary layer shape parameter, δ_3/δ_2
l_1	Length of bubble's laminar portion, $s_T - s_S$
l_2	Length of bubble's turbulent portion, $s_R - s_T$
R_c	Chord Reynolds number, $\rho U_\infty c/\mu$
R_{l_1}	Transition Reynolds number, $\rho U_S l_1/\mu$
R_{δ_2}	Momentum thickness Reynolds number, $\rho U \delta_2/\mu$
s	Coordinate along airfoil's surface from leading edge
t	Airfoil maximum thickness
u	Local mean velocity component tangent to airfoil's surface
u'	Local fluctuating velocity component tangent to airfoil's surface
U	External velocity tangent to airfoil's surface
U_∞	Freestream velocity
v'	Local fluctuating velocity in y-direction
x	Chordwise coordinate measured from leading edge
y	Coordinate normal to airfoil's surface
Δy	Thickness of separated shear layer, $y\|_{u/U=0.99} - y_{DS}$

Greek Symbols

δ	Boundary layer thickness, $y\|_{u/U = 1.00}$
δ_1	Boundary layer displacement thickness, $\int_o^\delta (1-u/U)dy$
δ_2	Boundary layer momentum thickness, $\int_o^\delta (u/U)(1-u/U)dy$
δ_3	Boundary layer energy thickness, $\int_o^\delta (u/U)[1-(u/U)^2]dy$
Λ_R	Horton's reattachment parameter, $[(\delta_2/U)(dU/ds)]_R$
μ	Absolute viscosity
ρ	Density
τ	Shear stress, $\mu\ \partial u/\partial y$ (laminar flow)
	$-\rho\overline{u'v'} + \mu\ \partial u/\partial y$ (turbulent flow)

Subscripts

DS	Dividing streamline
m	Mean value between transition and reattachment
o	Reference position
S	Laminar separation
T	Transition
R	Turbulent reattachment

Superscripts

$\overline{\quad}$	Time average

TABLE I Typical Freestream Turbulence Intensities in Percent.

	NUMBER OF FLOW RESTRICTORS		
R_C	0	1	2
200,000	0.160	---	---
160,000	0.129	—	—
140,000	0.108	0.167	0.296
100,000	---	0.147	---
80,000	---	0.134	---
50,000	—	0.125	0.220

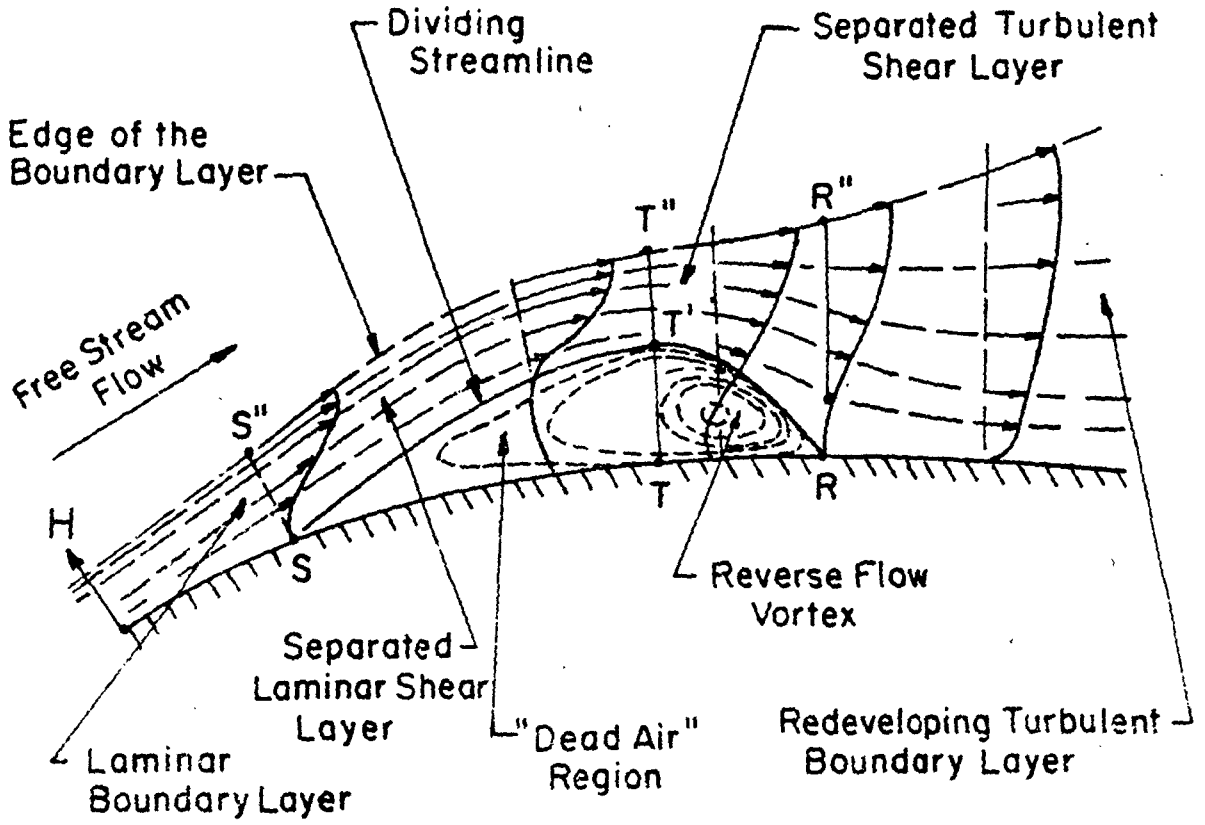

Figure 1. Sketch of a laminar separation bubble on an airfoil, Horton (Ref. 6)

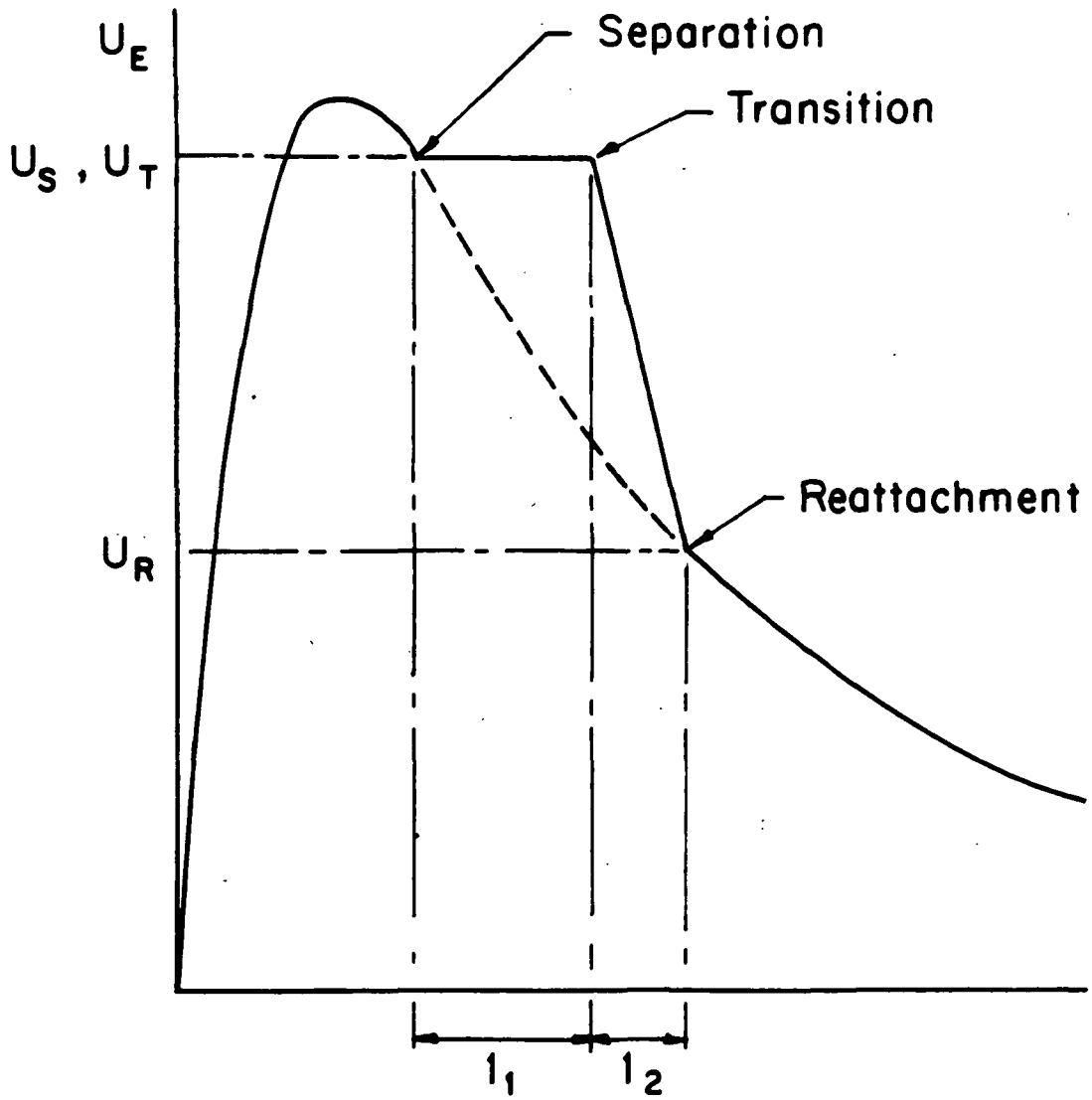

Figure 2. Horton's Assumed External Velocity Distribution in the Vicinity of a Separation Bubble

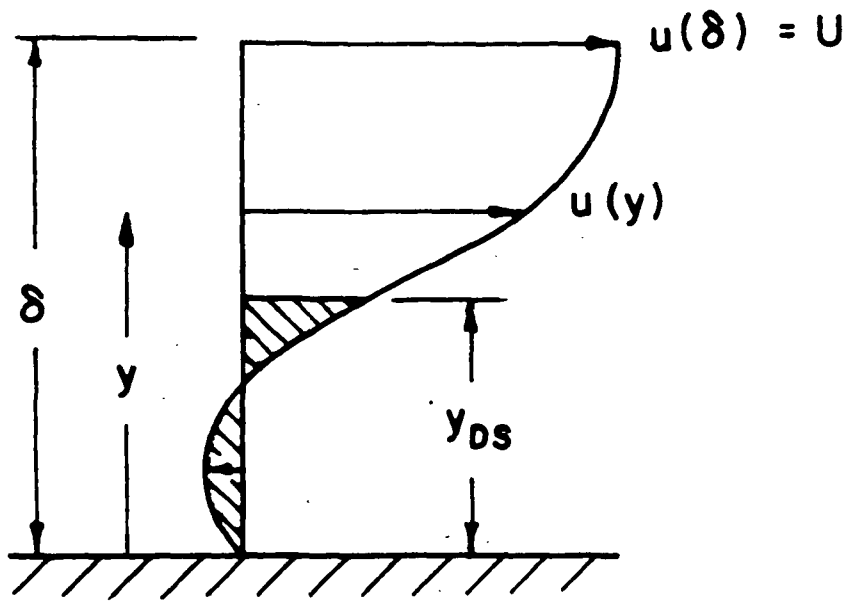

Figure 3. A Typical Velocity Profile with Reverse Flow

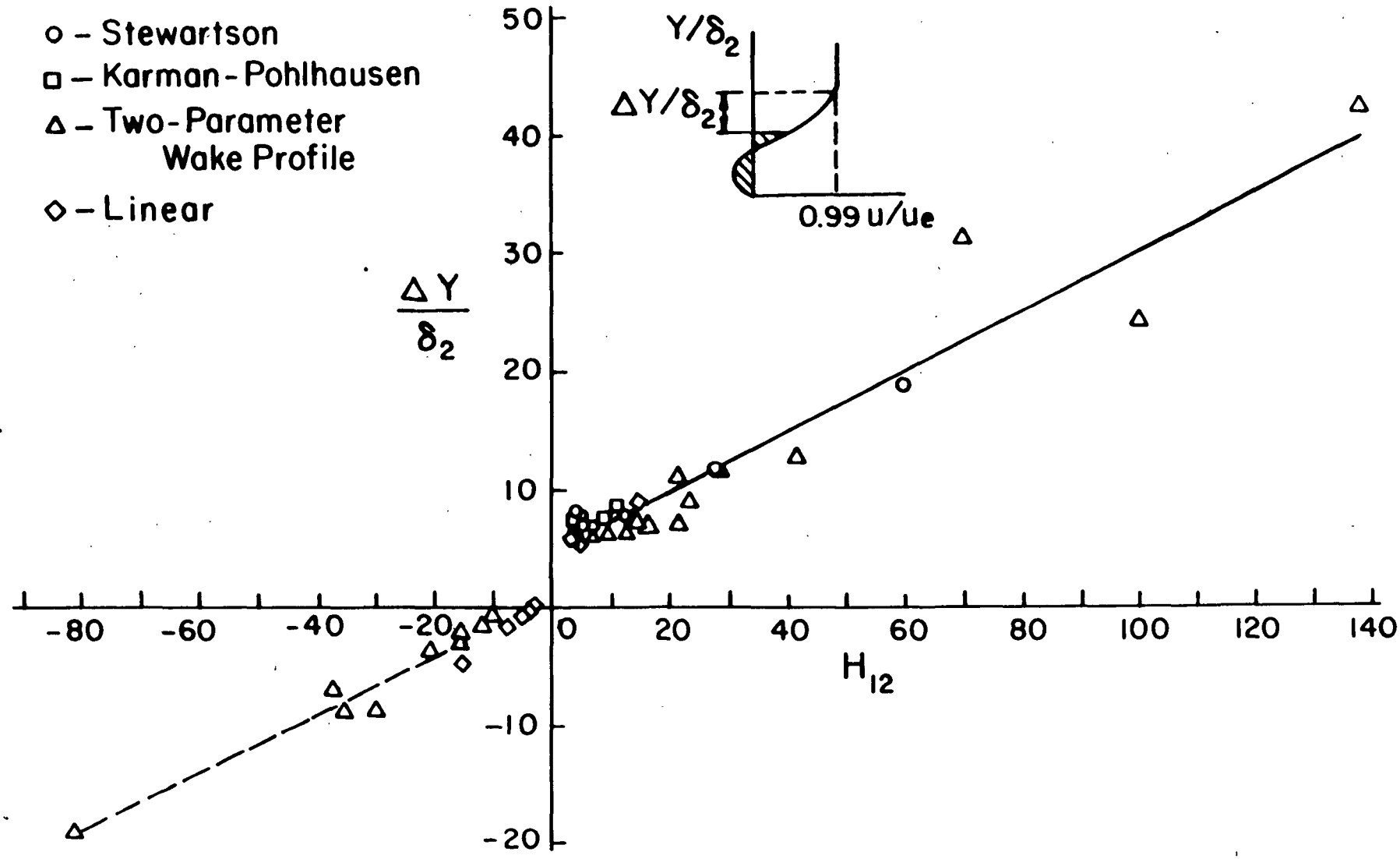

Figure 4. A Dividing Streamline Correlation for Velocity Profiles with Reverse Flow

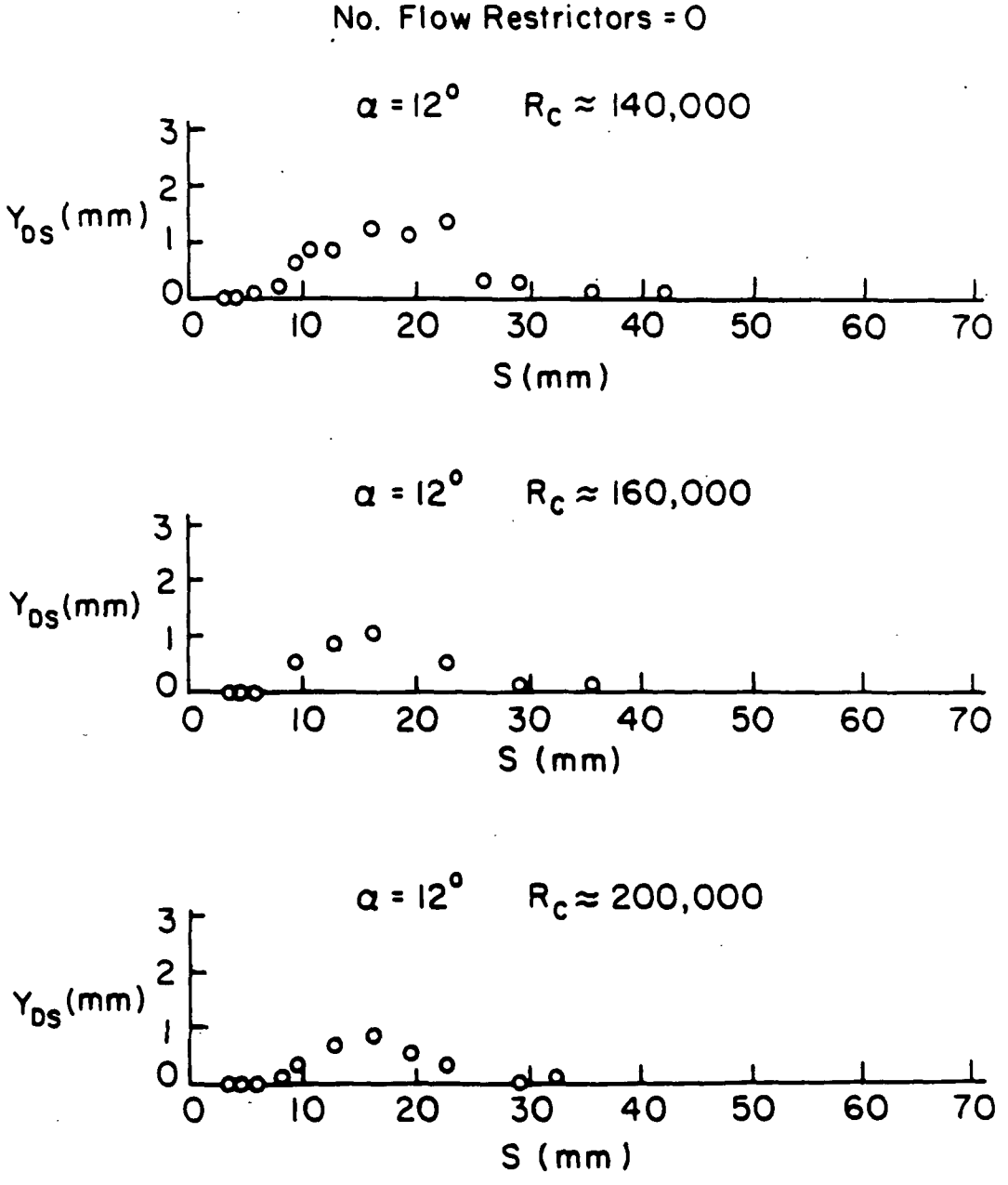

Figure 5. The Geometry of Separation Bubbles Formed on an NACA 66_3-018 Airfoil.

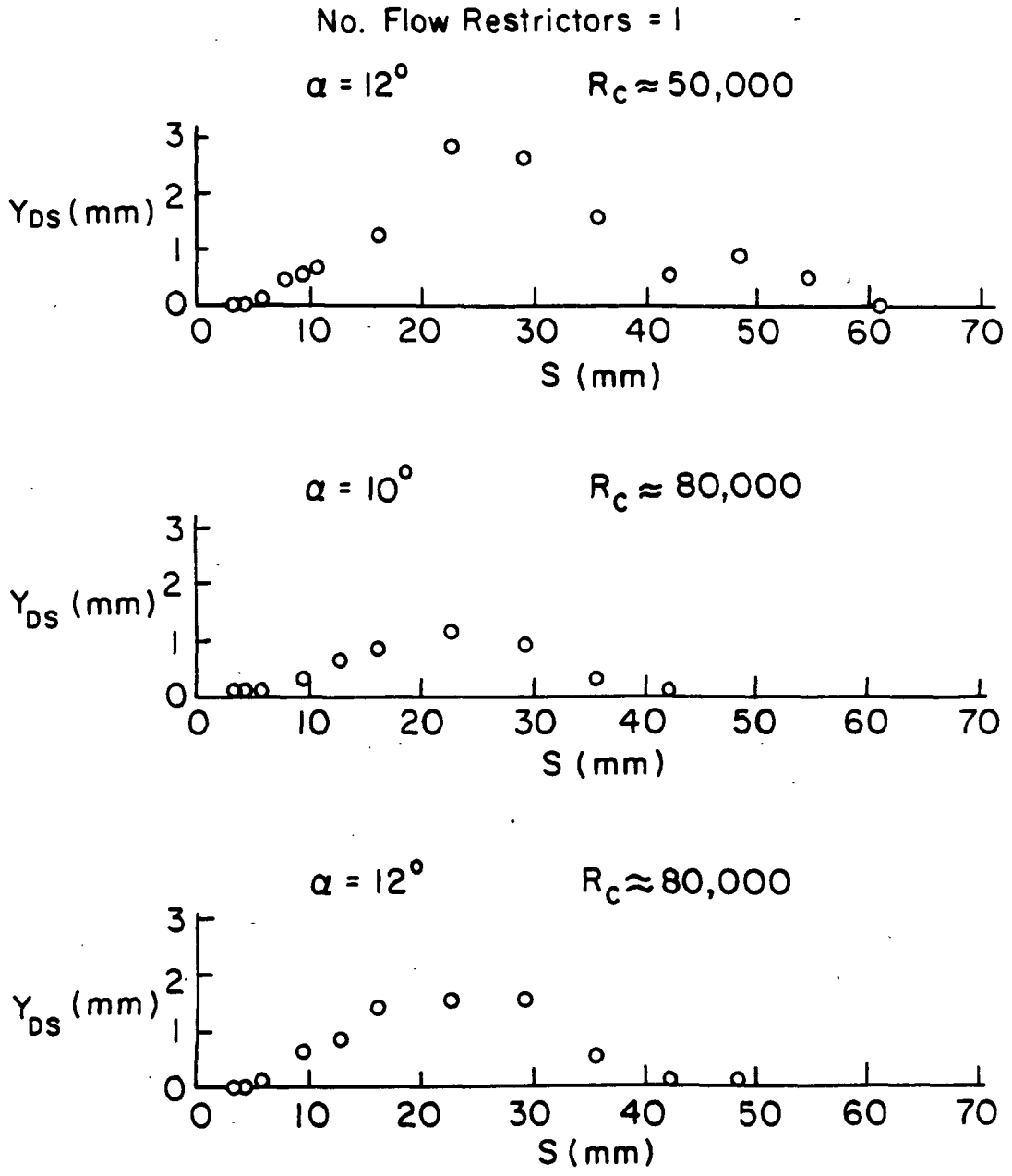

Figure 6. The Geometry of Separation Bubbles Formed on an NACA 66_3 -018 Airfoil with One Flow Restrictor Present

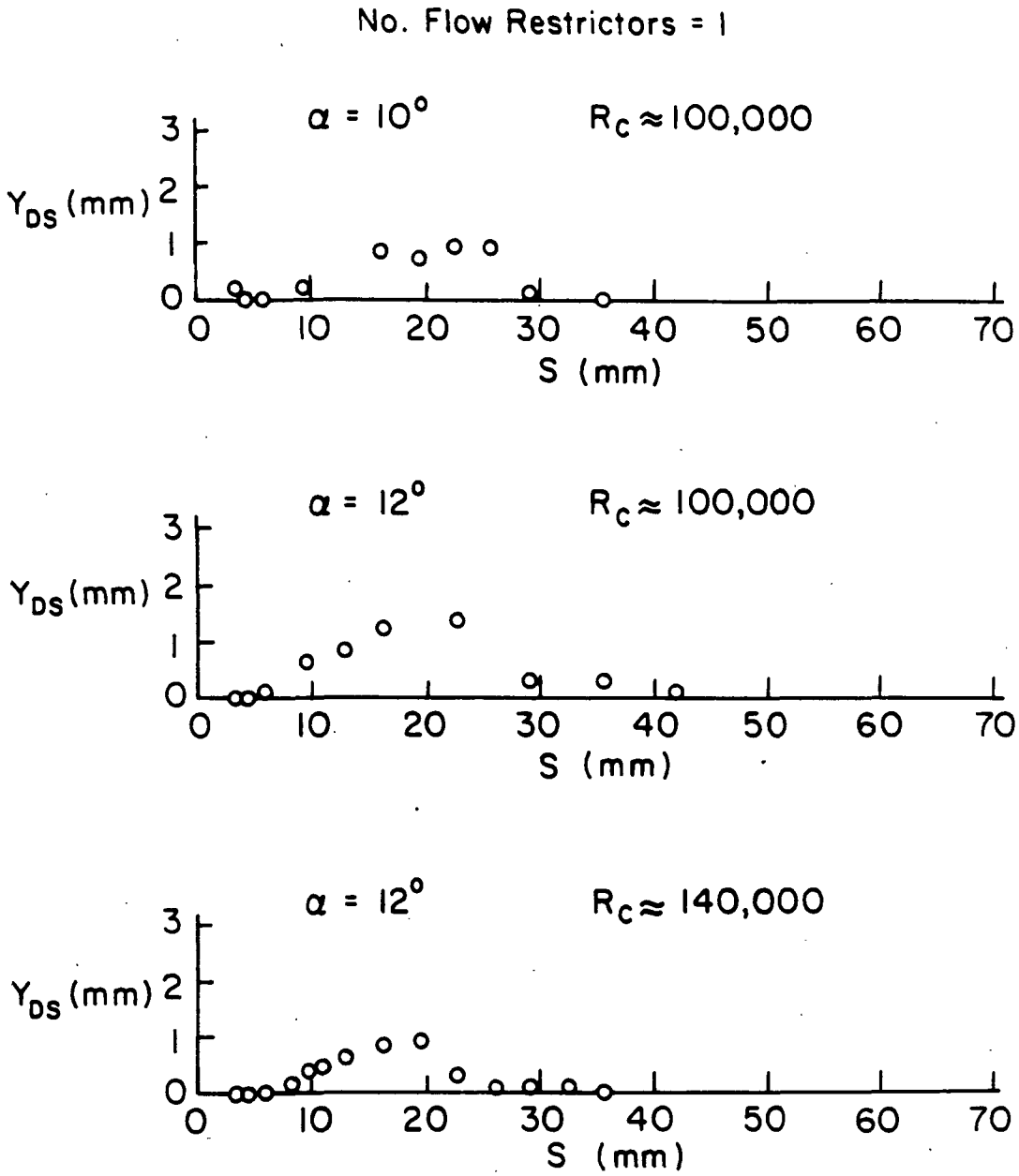

Figure 7. The Geometry of Separation Bubbles Formed on an NACA 66_3-018 Airfoil with One Flow Restrictor Present

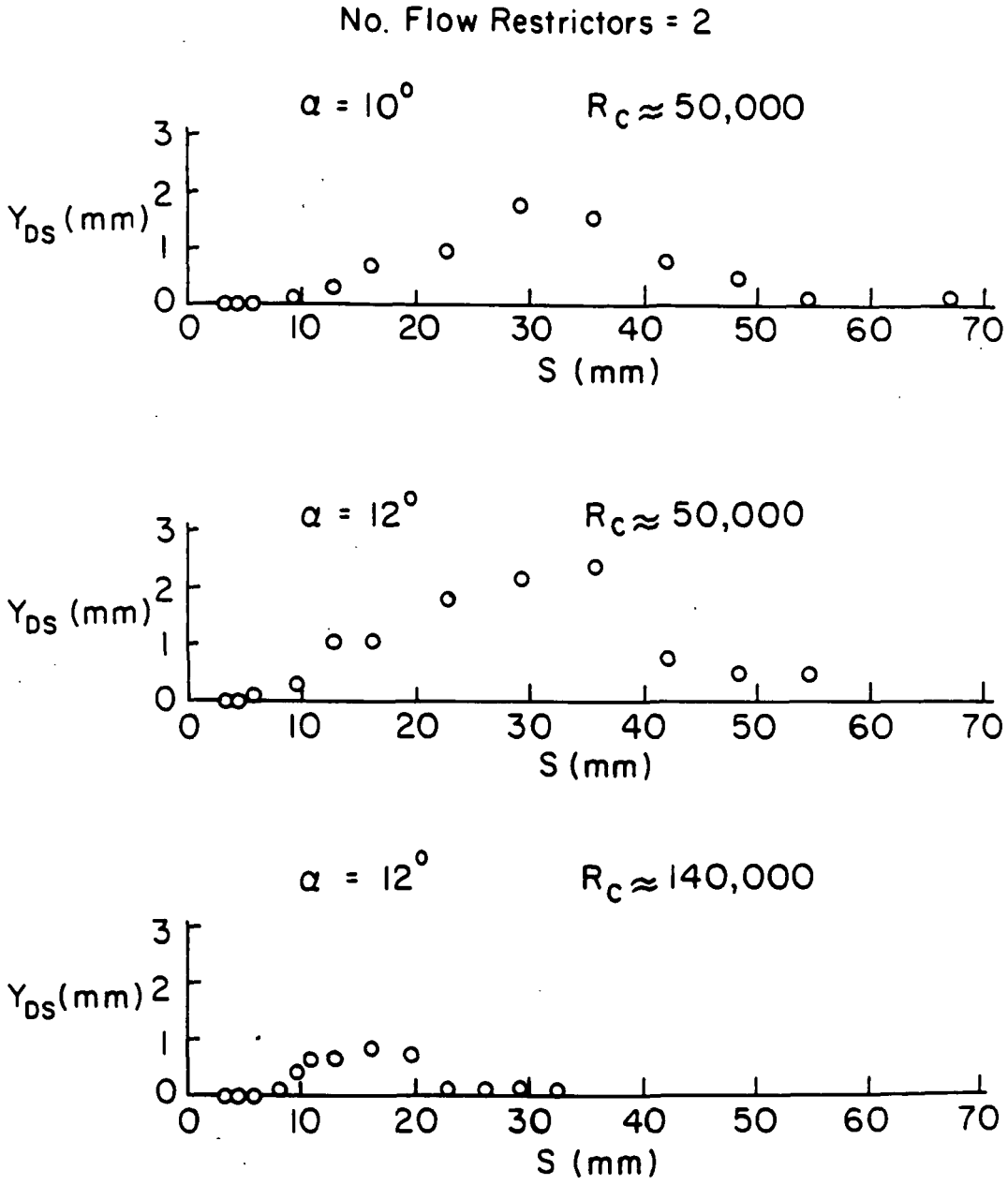

Figure 8. The Geometry of Separation Bubbles Formed on an NACA 66_3-018 Airfoil with Two Flow Restrictors Present

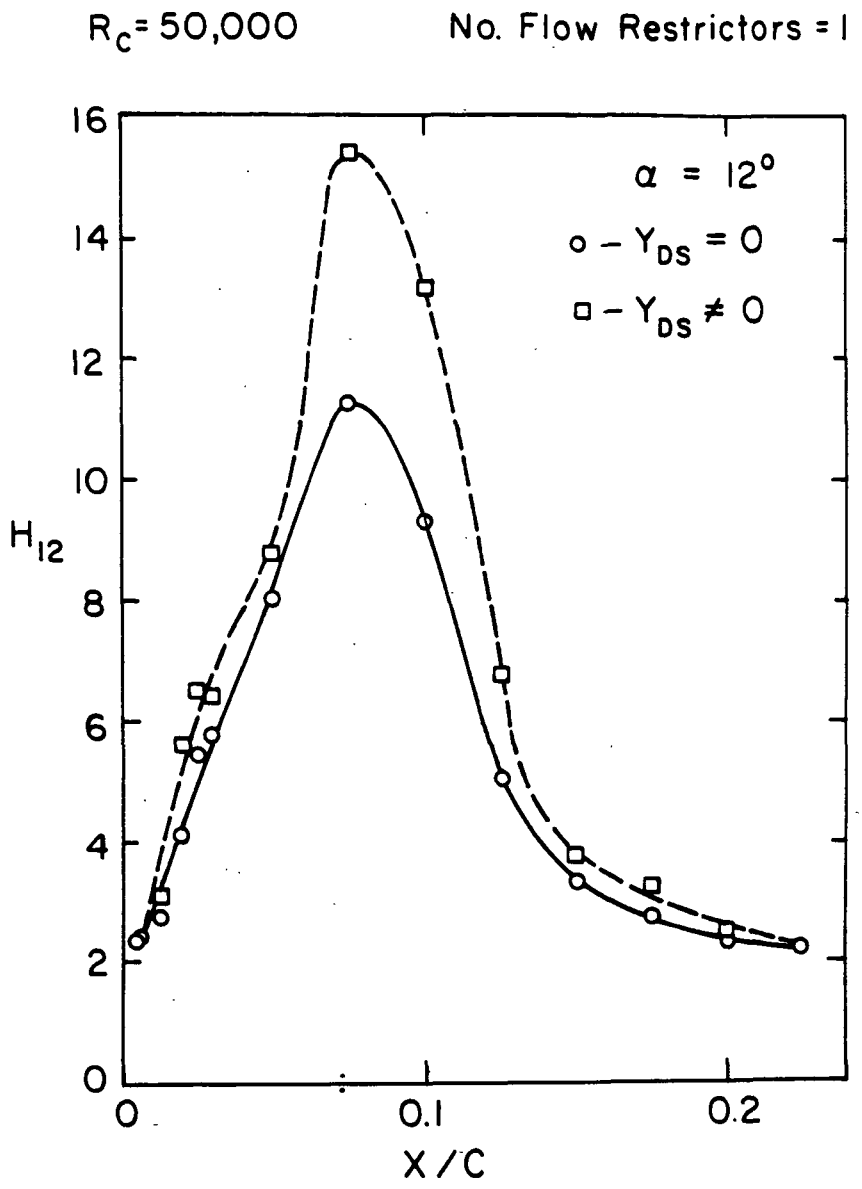

Figure 9. The Effect on H_{12} of Accounting for Reverse Flow within a Separation Bubble

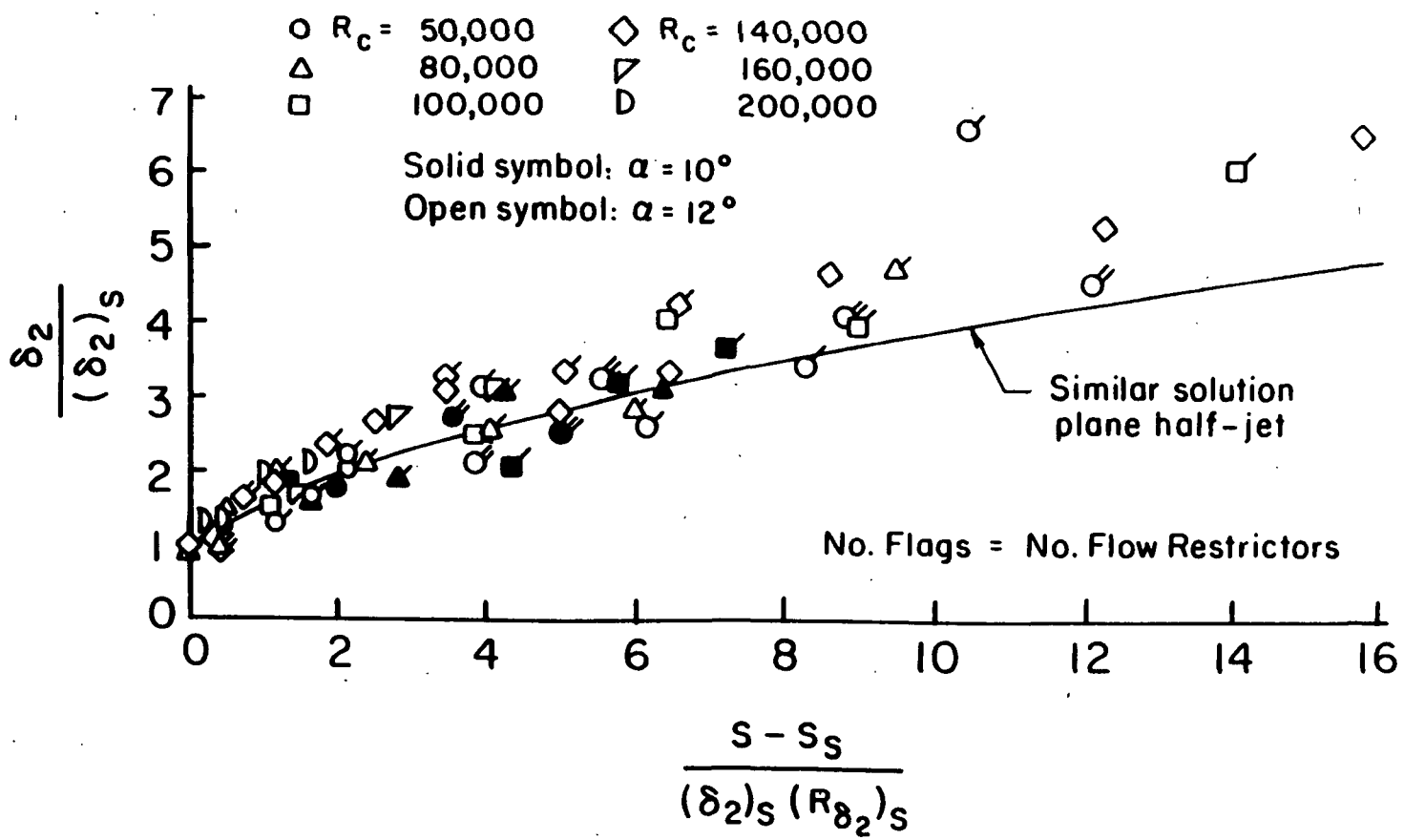

Figure 10. Momentum Thickness Correlation for Flow within a Separation Bubble's Laminar Portion

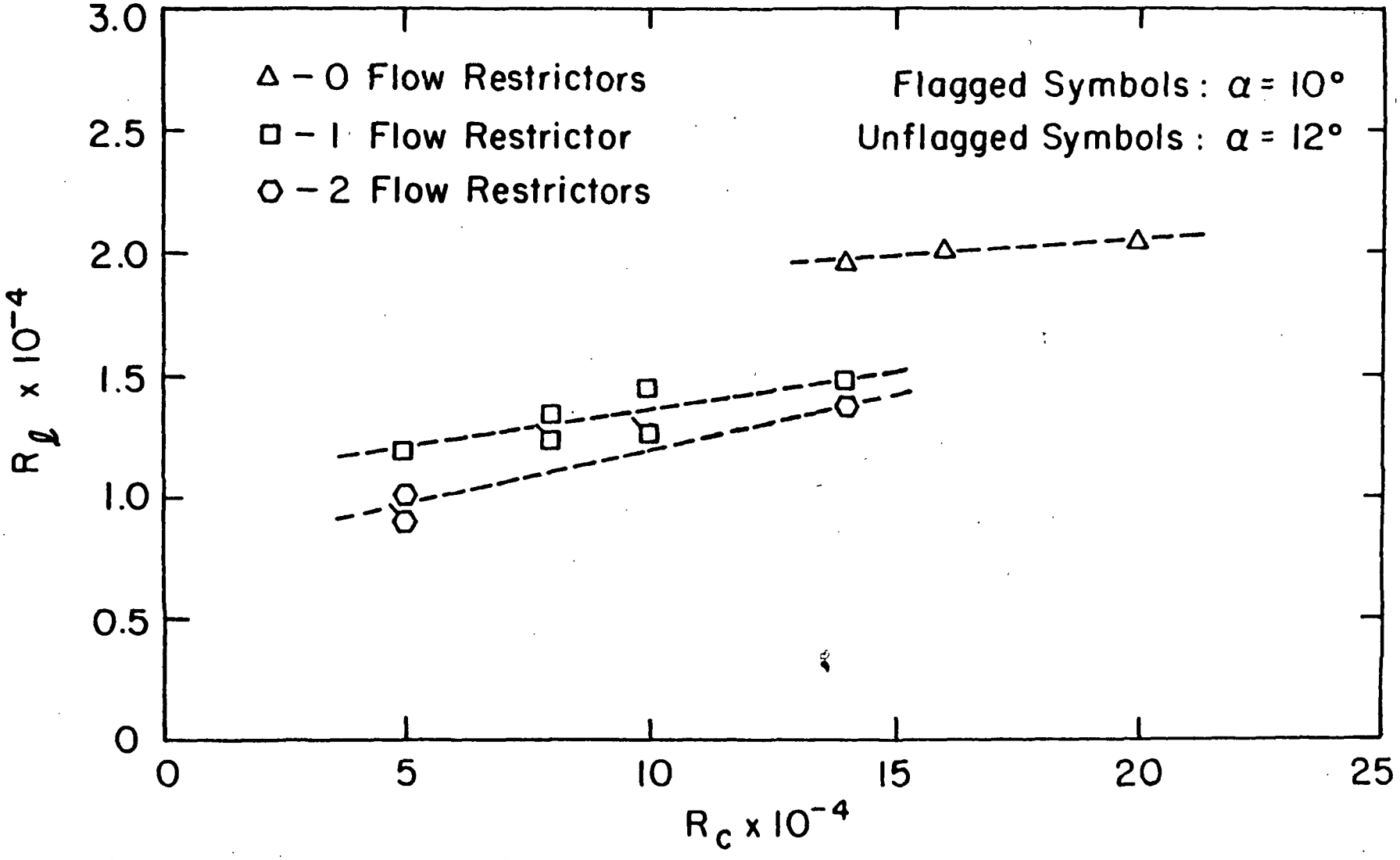

Figure 11. The Effect of the Chord Reynolds Number on the Transition Reynolds Number

$$(C_d / H_{32})_m = 0.0121$$

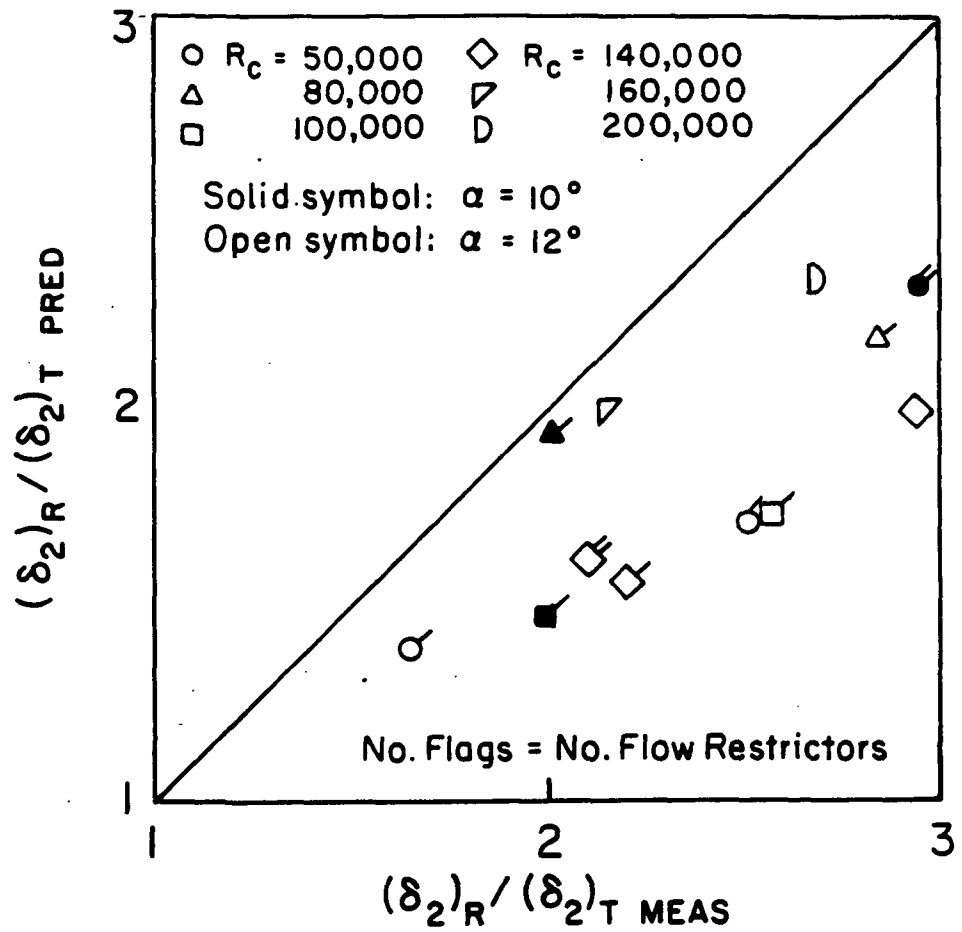

Figure 12. Momentum Thickness Growth Over a Bubble's Turbulent Portion: Measured Versus Predicted, with $(C_d/H_{32})_m$ = 0.0121

$$(C_d/H_{22})_m = 0.0233$$

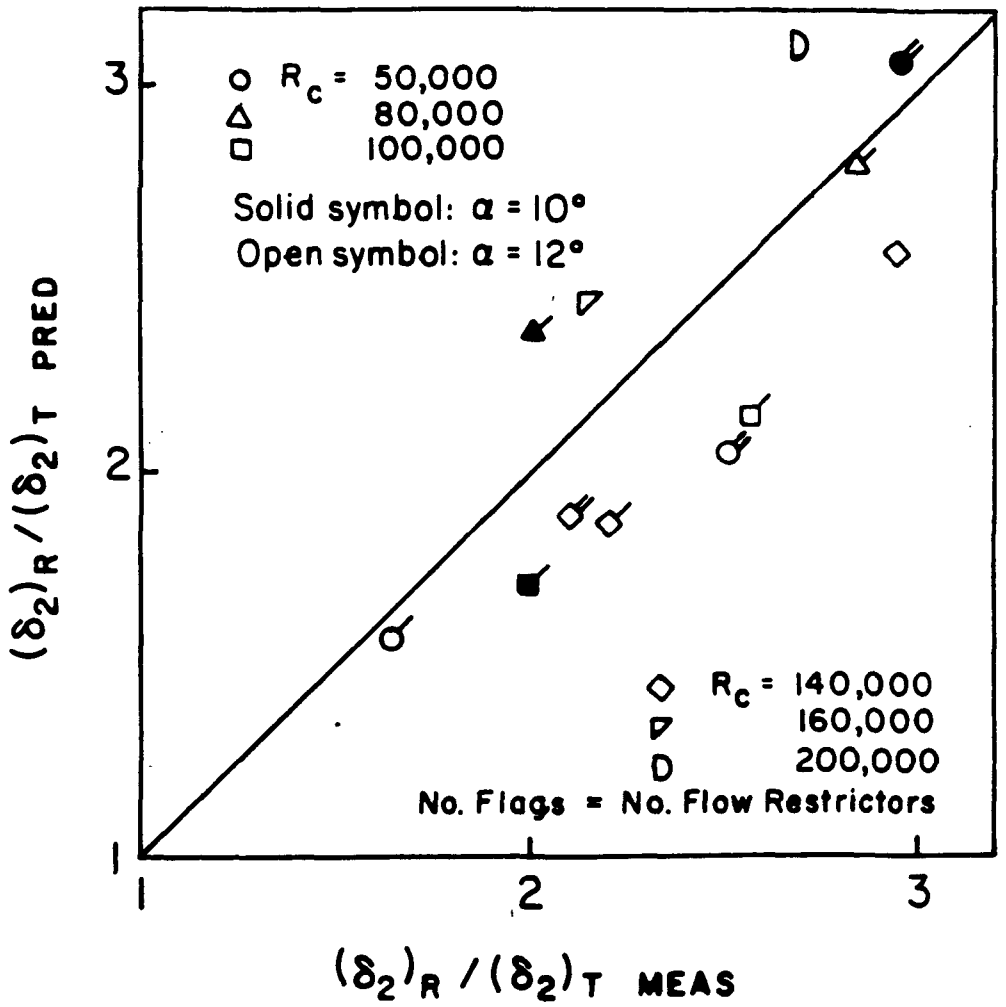

Figure 13. Momentum Thickness Growth Over a Bubble's Turbulent Portion: Measured Versus Predicted, with $(C_d/H_{32})_m$ = 0.0233

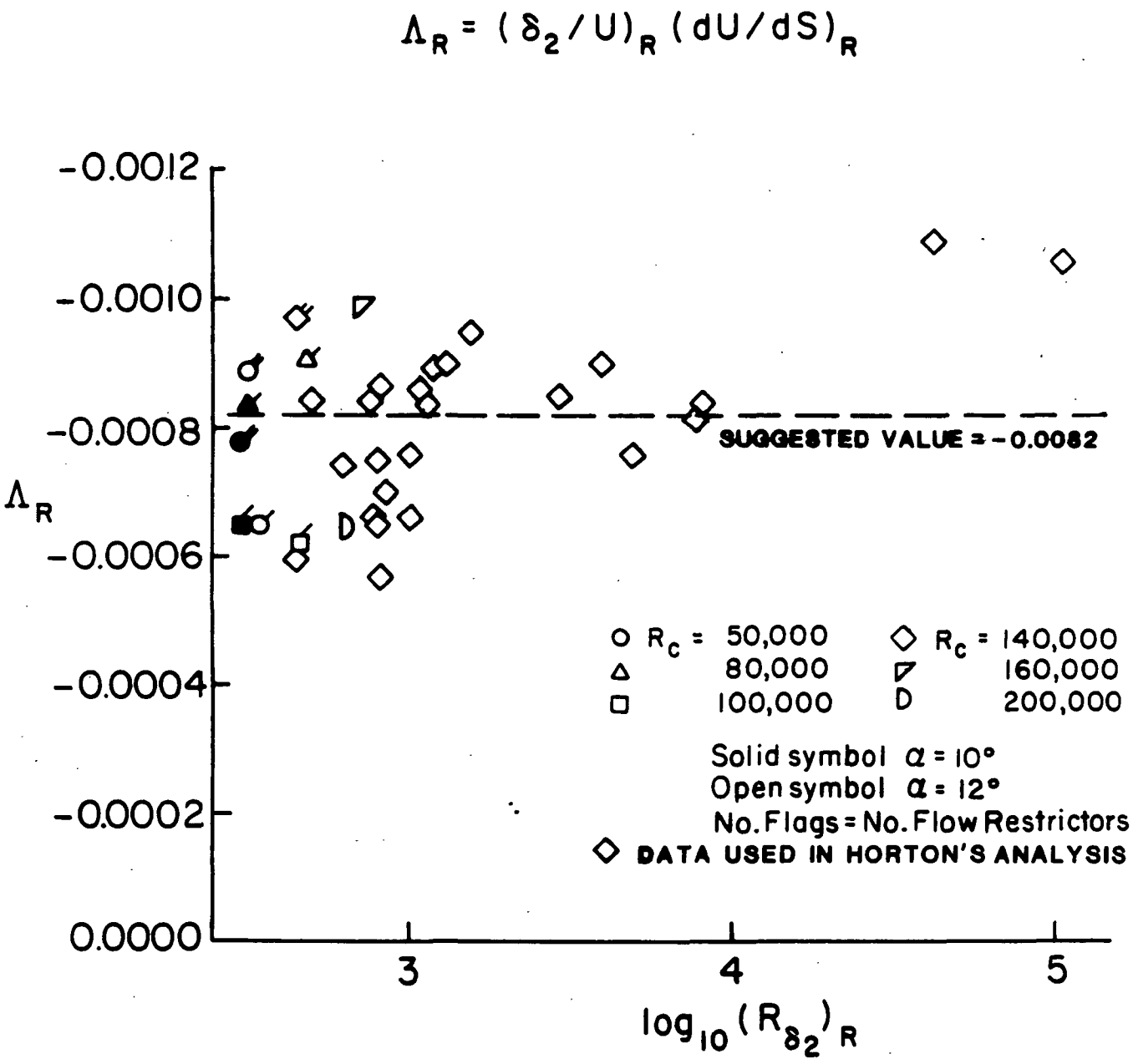

Figure 14. Horton's Reattachment Criterion

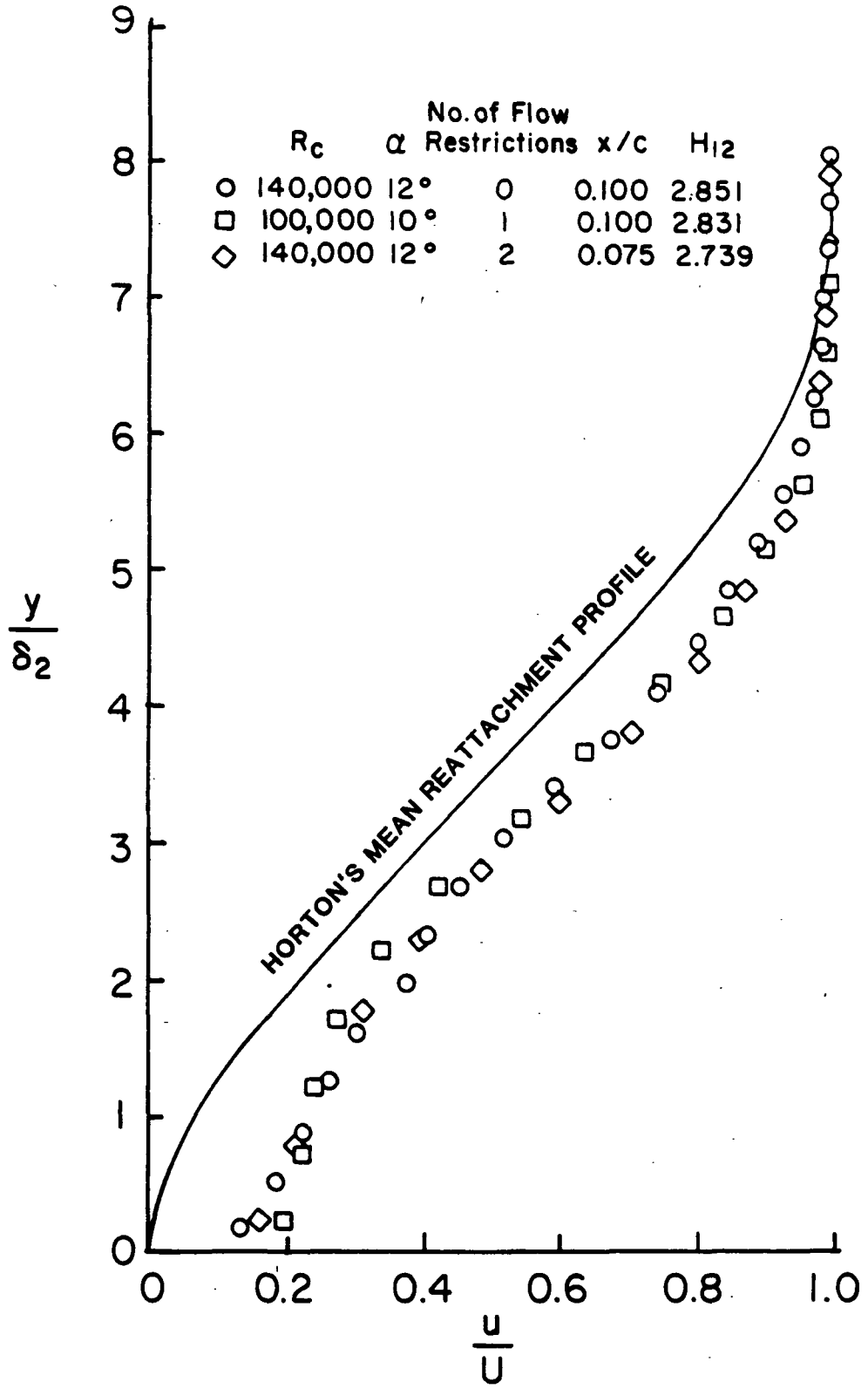

Figure 15. Velocity Profiles Measured Near the Reattachment Point

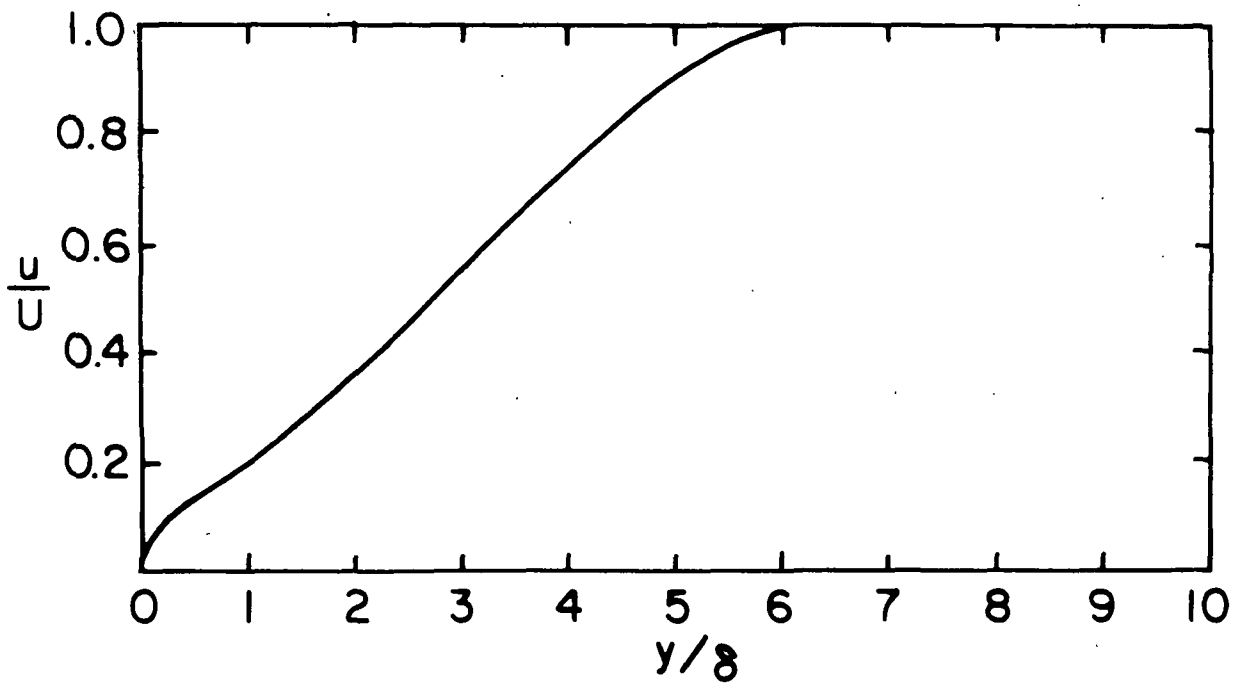

Figure 16. A Typical Turbulent Separation Profile (Reference 12)

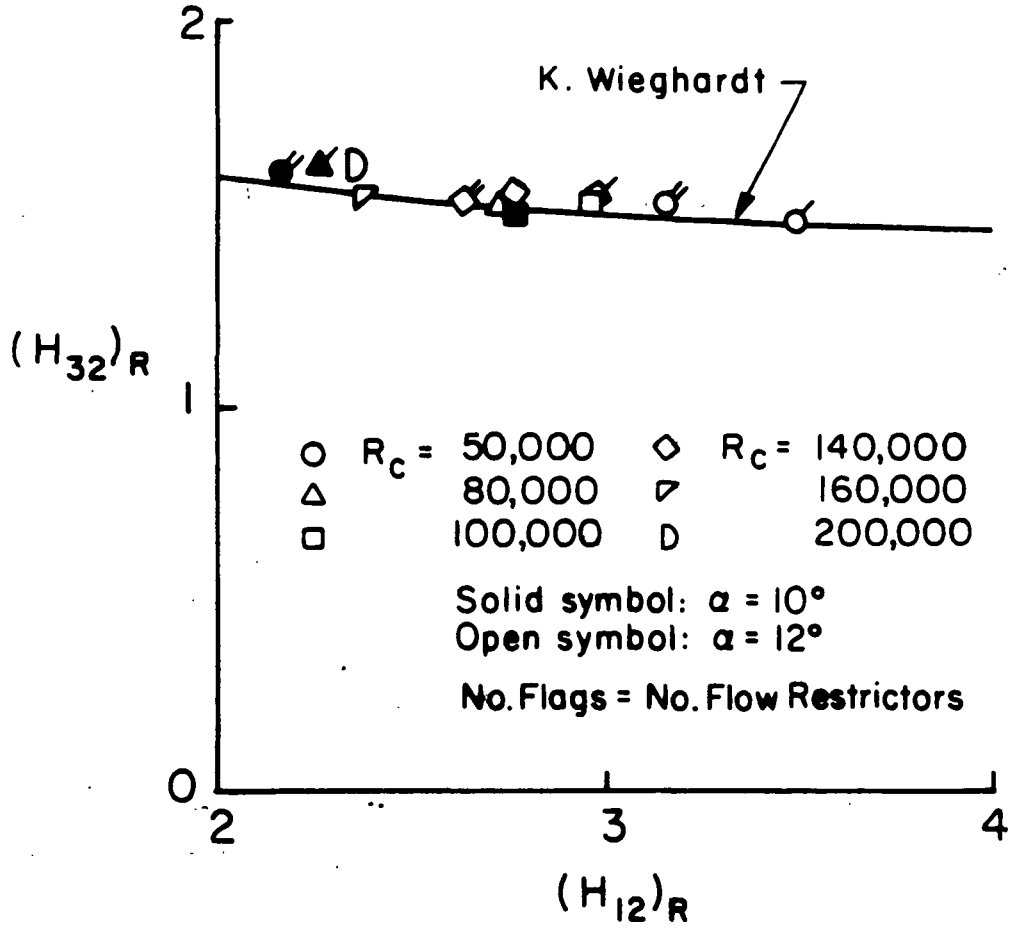

Figure 17. Reattachment Shape Factors